TIPS: Trajectory Inference of Pathway Significance through Pseudotime Comparison for Functional Assessment of single-cell RNAseq Data

Running title: scRNAseq pathway inference

Zihan Zheng[2,3], Xin Qiu[4], Haiyang Wu[4], Ling Chang[5], Xiangyu Tang[1], Liyun Zou[5], Jingyi Li[6], Yuzhang Wu[5], Jianzhi Zhou[2], Shan Jiang[7,#], Ying Wan[1,#], Qingshan Ni[1,#]

[1] Biomedical Analysis Center, Army Medical University, Chongqing, China

[2] Biowavelet Ltd., Chongqing, China

[3] Chongqing International Institute for Immunology, Chongqing, China

[4] R&D Department, TCRCure Ltd., Chongqing, China

[5] Department of Immunology, Army Medical University, Chongqing, China

[6] Department of Rheumatology and Immunology, First Affiliated Hospital of Army Medical University, Chongqing, China

[7]Institute for Advanced Study, Shenzhen University, Shenzhen, China

[#]Co-corresponding authors

Please address any correspondence to:

Ying Wan
wanying516@foxmail.com
Director, Biomedical Analysis Center
Army Medical University
Chongqing, China

Qingshan Ni
qingshanni@foxmail.com
Biomedical Analysis Center
Army Medical University
Chongqing, China

Shan Jiang
shan.jiang1975@szu.edu.cn
Institute for Advanced Study
Shenzhen University
Shenzhen, China

Biographical note

Y.W. is the director of the Biomedical Analysis Center at Army Medical University and has led work focused on single cell sequencing and vesicular transport.

Q.N. is a bioinformatician and lecturer at Army Medical University whose main research focus is on data analysis for high-throughput sequencing.

S.J. is an assistant professor at Shenzhen University working in the field of T cell development and differentiation.

Z.Z. is a bioinformatician working on biological applications of trajectory analysis.

X.Q. is a technician specializing in performing and optimizing methods for single-cell library construction

H.W. is a bioinformatician working on identifying antigen-specific T cell clones through single-cell sequencing

L.C. is a PhD student at Army Medical University working on applying scRNAseq to interrogate T cell differentiation and clonal behavior in autoimmune diseases

X.T. is a PhD student at Army Medical University working on applying scRNAseq to identify new mechanisms involved in osteoclast differentiation

L.Z. is an assistant professor at Army Medical University working in the fields of antigen presentation and autoimmunity

J.L. is a clinician and assistant professor in the Department of Rheumatology and Immunology who specializes in autoimmune diseases and has projects focused on exploring the impact of pharmaceutical intervention on immune response

Y.W. is the director of the Immunology Institute at Army Medical University who specializes in T cell immunology during autoimmunity and chronic infection

J.Z. is the research director at Biowavelet Ltd., a company working on developing hardware and software for automation of high-throughput sequencing library construction

Abstract

Recent advances in bioinformatics analyses have led to the development of novel tools enabling the capture and trajectory mapping of single-cell RNA sequencing (scRNAseq) data. However, there is a lack of methods to assess the contributions of biological pathways and transcription factors to an overall developmental trajectory mapped from scRNAseq data. In this manuscript, we present a simplified approach for trajectory inference of pathway significance (TIPS) that leverages existing knowledgebases of functional pathways and transcription factor targets to enable further mechanistic insights into a biological process. TIPS returns both the key pathways whose changes are associated with the process of interest, as well as the individual genes that best reflect these changes. TIPS also provides insight into the relative timing of pathway changes, as well as a suite of visualizations to enable simplified data interpretation of scRNAseq libraries generated using a wide range of techniques. The TIPS package can be run through either a web server, or downloaded as a user-friendly GUI run in R, and may serve as a useful tool to help biologists perform deeper functional analyses and visualization of their single-cell and/or large cohort RNAseq data.

Keywords: trajectory mapping; pseudotime; TIPS; pathway analysis

Introduction

Recent advances in single cell RNAseq (scRNAseq) library construction technologies, coupled with decreases in cost of high-throughput sequencing, has led to a proliferation of new single cell transcriptome data across a range of species and developmental/disease contexts. In order to interpret this data, a slew of new bioinformatics tools and analysis techniques have been developed. These include network-based methods to infer cis-regulatory interactions, splicing-informed mapping of RNA-velocity, and inferences on key intercellular interactions based on receptor-ligand pairs [1-3]. These and other novel tools have helped to unlock the potential of scRNAseq to provide a plethora of information that was previously inaccessible to bulk sequencing-based approaches.

However, one area in which currently available single-cell analysis tools are lacking in is in pathway analysis. While pathways analysis and similar gene-set based enrichment analyses are among the most common ways to infer molecular mechanisms that are involved in the altered cellular behavior under different conditions, directly applying bulk-sequencing inspired pathway analysis methods to scRNAseq data comes with substantial difficulties. Unlike bulk sequencing profiles, scRNAseq transcriptome tend to be dropout-heavy, with technical variation causing false-zero detection of any given gene in a cell [4-5]. Chance-driven technical dropout also tends to be particularly severe for genes with low- to medium- expression magnitudes, many of which are typically included as key components of biological pathways. Because of this, some approaches (such as Metacell) have been developed to enable gene set enrichment analyses across clusters of cells using composite profiles [6]. Other tools, such as AUCell and GSVA, can generate scored profiles for single cells along a given pathway of interest, but is predominately applied to identify differentially regulated pathways between two clusters of interest [7-8]. This emphasis on pairwise differential regulation is less suitable for single cell datasets that encompass multiple cellular states and functional clusters. Furthermore, these approaches cannot provide information on the temporal order by which pathways may change during a larger biological process.

In order to implement pathway analysis on a single-cell level, we present here a novel analytical framework that provides trajectory inference of pathway significance (TIPS). Our approach leverages the common trajectory mapping principle of pseudotime assignment to build pathway-specific trajectories from a pool of single cells. The pseudotime values for each cell along these pathway-specific trajectories are then compared to identify the processes with highest similarity to an overall trajectory in a simple and intuitive process. Key genes that are associated with both the overall trajectory and/or pathway-specific trajectories are also identified, providing ready targets for downstream validation work. Direct visualizations are also offered at each of the primary steps, with customizable options for figure generation for pathways and genes of interest. The key modules in TIPS incorporate in a number of leading scRNAseq analysis tools, and can be run sequentially within a shiny GUI in R with the source code available on GitHub, or on a dedicated webserver. We hope that the TIPS workflow may help

further expand the range of functional analyses that are possible when working with scRNAseq data, and help derive new functional insights into complex biological processes.

Materials and Methods

Overview of the TIPS framework

The TIPS framework is designed as 7 primary modules (described in detail below) intended to be run sequentially in R as either a local shiny-based GUI, or as online as a webserver. Each module will automatically generate and format the analysis results as necessary to permit further analyses without a need for manual modification. A schematic overview of these modules is included as Figure1.

Uploading Data

TIPS takes as its primary data input a standard gene expression matrix, wherein each row corresponds to a gene and each column a cell, from a comma-delimited (.csv) file. Ideally, this matrix should be pre-processed beforehand to only include in the cells that are of sufficient quality and which are pertinent to the intended trajectory analysis. Since preprocessed data may have been pre-normalized, an option is available to either log-normalize raw data, or to accept it as is. TIPS also accepts metadata information for each cell (regarding sample quality, origin, type, etc), from an additional (.csv) file for further visualizations. The user may then choose a list of gene sets to consider from a dropdown menu (6 are built-in, including Reactome, KEGG, BioCarta, Msigdb), or otherwise upload an additional (.gmt) file containing the gene lists they wish to analyze [9-11]. This allowance for built-in options allows for customized analysis of data derived from other organisms or knowledgebases.

Dimension Reduction

TIPS automatically loads and manages the data input as a Seurat object, and runs three different dimension reduction algorithms (PCA, tSNE, and UMAP) to generate 2-D visualizations of the transcriptome similarity between cells [12-13]. Users may select cutoff parameters for selecting the list of highly variable genes to consider for these reductions (both expression and dispersion cutoffs), and number of nearest neighbors, in order to optimize the analysis to suit their dataset. The results from the reduction can be visualized directly, with metadata information as selectable overlays, while a Louvain clustering algorithm is run at common resolutions to provide a range of clustering results.

Primary Trajectory Analysis

To generate the primary trajectory of the dataset, the same pool of highly variable genes used for dimension reduction in the previous step is passed to Monocle for DDRTree-based mapping and pseudotime assignment [14]. Since the actual assignment direction for pseudotime values can be arbitrary, an option to reverse the initial order of cells is provided, such that users may select an

order more intuitive for their question of interest in terms of expected temporal relations between clusters. This assignment is then treated as the reference pseudotime trajectory for downstream analysis.

Pathway Inference

In order to identify the pathways that are functionally associated with the overall trajectory of interest, we first load into the TIPS pipeline the selected reference knowledgebase of pathways for consideration. We then tailor these reference pathways to the dataset of interest to remove genes with missing expression, and prune out overly small pathways based on absolute size (<20 genes). TIPS then iteratively runs the DDRTree algorithm to generate one trajectory per pathway of interest, considering all of the expressed genes from the pathway (including ones where the genes display non-significant variation in expression) to give a complete picture of pathway dynamics. This process reduces each pathway to a single linear vector of pseudotime values. These pseudotime vectors are then compared to the reference pseudotime trajectory using absolute Pearson's correlation to assess relative similarity in terms. Notably, absolute comparisons are used for these measures to avoid potentially misleading inferences about the direction of trajectory values. In order to assess the pathways with true significance, DDRTree is also iterated on randomly generated pathway lists to establish a false discovery rate for genes sets of a given size. Pathways at correlation levels below 5% FDR and which have significant correlation in terms of absolute gene expression (> 0.6) are considered to be significantly associated with the overall trajectory.

Pathway Temporal Alignment

Individual significantly associated pathways may have distinct modes of behavior over the course of the pseudotime trajectory, with some showing rapid changes early on, while others are late-breaking. In order to provide a temporal understanding of these pathway dynamics, we further utilized the switchde package in R to help identify genes with switch-like expression characteristics [15]. We can then visualize the distribution of switch points with respect to pseudotime for each individual pathway, and subsequently compare these distributions to generate a temporal alignment.

SOM-based Pathway Selection

Although the absolute order of pseudotime values may be arbitrarily assigned and is not dependent upon a unidirectional change in expression within a given gene list, researchers may be interested in focusing on investigating processes that do show continual increases or decreases expression over time. In order to accommodate this need, we implemented self-organizing maps (SOMs) to cluster the cells using the kohonen package in R [16]. Users can select their pathways of interest from a dropdown menu to assess the direction, while also choosing the number of nodes for the SOM that would best fit their interest. Pathways that display monotonic changes in

behavior can thus be visualized in this manner. The SOM can also be used to help visually distinguish pathways with more complex expression kinetics.

Individual Gene Selection

Although the approach outlined above is sufficient for identifying pathways that meaningfully contribute to an overall trajectory, it is oftentimes necessary to further clarify the exact genes that drive such a contribution. To address this question, we included three distinct methods for identifying critical genes within a pathway. First, we consider the genes with switch-like behavior recovered from switchde, as the singular and abrupt change in expression within these genes make them good candidates for functional screening and validation. Second, since other critical genes may display milder and monotonic changes in expression, we also compute the Pearson correlation between gene expression and pseudotime progression to help identify genes not found by switchde. Finally, since still other factors may display more complex changes in expression dynamics (alternating increases and decreases, or the like), we further weigh the relative contribution of a given gene on the pseudotime correlation of its parent pathway. Through these three distinct approaches contained in our final module, we can subsequently narrow down the range of candidate genes to consider for further validation work.

Analyzed Datasets

For our initial analysis of a simulated dataset, we used the splatter package in R with default setting to generate a dataset of 500 cells with 5,000 expressed genes per cell [17]. To enable analysis of the impact of technical dropout, we further used the dropout function in splatter to add in zero-inflation up through a range of median expression values.

scRNAseq Library Construction and Sequencing

In order to provide a direct demonstration of the use of the TIPS framework on real scRNAseq data, we isolated peripheral blood mononuclear cells (PBMCs) from whole blood provided by a healthy donor under approval of the Ethics Committee of Southwest Hospital as part of a pilot study. CD8+ T cells were acquired and FACS-sorted (Beckmann Coulter) into a 96-well plate following staining with antibodies against CD3, CD4, and CD8 (BD). Cells were then lysed, and libraries were prepared using the scSTATseq workflow that we have previously developed [18]. Libraries were sequenced using the HiSeq 4500 platform (Illumina) and preprocessed as previously described. Alignment-free counting of reads relative to the reference human transcriptome was performed using Salmon [19]. The resulting gene expression matrix was then read into the Seurat package in R, where quality control filtering was performed to remove cells with excess mitochondrial reads (>10% of all reads), as well as outliers in terms of number of genes recovered (<5000 or >15,000). The remaining 69 libraries were then passed to the TIPS framework for further analysis and visualization.

Additional Comparison Datasets

Additional data from scRNAseq libraries constructed using alternative methods were obtained from GSE133535, a benchmarking study of different library construction protocols [20]. Since a mix of cells were used in the study, we individually downloaded each of the data matrices corresponding to a single method, and filtered them based on metadata annotation to only retain human cells. Data on these cells was then loaded into Seurat for UMAP-based clustering in order to identify clusters of CD8+ T cells (based on positive expression of CD8, CD3D, and lack of expression of CD4 and NCAM1). Transcriptome information from these CD8+ T cells were then passed to TIPS for additional analysis.

For analysis of single CD8+ T cells from HCC patients, fully processed sparse matrix files were obtained from GSE98683, and annotated CD8+ populations were used for further analysis through TIPS [21]. Data for the HCC samples treated with immune checkpoint blockade was similarly processed from GSE125449 [22].

Results

Testing of the TIPS workflow using simulated data

In order to assess the robustness of the analysis workflow described, we first simulated a medium-sized scRNAseq dataset of 5,000 genes and 500 cells ordered along a single path. We then compared the performance of different correlation metrics for comparing pathways to a common trajectory using 1,000 randomly selected gene lists and 100 highly variable gene (HVG) lists. Since the baseline pseudotime trajectory was generated based on a complete list of HVGs, we anticipated that subsets of the HVG list would show true signal, while the completely random lists would reflect the range of noise. Interestingly, we observed that the HVG lists were essentially indistinguishable from random background when mean pathway gene expression level was considered (Fig2A). However, pseudotime-to-pseudotime correlations showed a clear separation between HVG lists and background (Fig2B).This phenomenon suggested that the TIPS workflow will highlight pathways as being highly significant regardless of average expression (Fig2C). Instead, we observed that the constituent genes from the highly correlated lists displayed balanced distribution, with a similar number of genes having increasing or decreasing expression (and changes of similar magnitude) over the course of the pseudotime trajectory (Fig2D). This trend could also be clearly identified in terms of specific genes from a single pathway (Fig2E). At the same time, we also observed a clear pattern wherein the addition of additional information from more HVGs led to higher correlation with the overall pseudotime (Fig2F). As such, these results suggest that pseudotime correlation provides a sensitive method for comparing two trajectories, by accounting for genes with both increasing and decreasing expression.

At the same time, we also assessed the potential influence of other factors on the accuracy of pseudotime mapping to clarify its range of applicability. Since scRNAseq libraries

may vary greatly in terms of number of cells recovered, genes recovered, and in sequencing quality, we controlled for each of these factors in turn. Interestingly, pseudotime mapping using subsampled cells demonstrated that decreasing the size of the dataset did not have a strong of an effect on correlation accuracy, such that a correlation above 0.9 could be maintained even when the dataset was downsampled to 10% of its original size (Fig2G). However, the gene detection quality of the cells sequenced had a substantial impact on accuracy, as increasing the degree of technical dropout in the data led to a clear deterioration in the correlation (Fig2H). This deterioration demonstrates that pseudotime assignment is sensitive to information loss. In a similar vein, we observed that the number of genes considered for pseudotime assignment also had significant influence on its accuracy; larger sets of randomly selected genes tended to have significantly higher background noise than their smaller counterparts (Fig2I). Since a given dataset may only feature significant expression in a subset of all genes assigned to a given pathway, the relative size and representation rate of a pathway may also influence correlation interpretation. As such, we elected to run independent calculations of background noise using random lists for each pathway in order to control for differences in gene list size and representation.

TIPS confirms existing knowledge of CD8+ T cell differentiation

To validate the utility and biological relevance of our workflow, we then analyzed 69 single-cell libraries of peripheral blood CD8+ T cells from a healthy donor using the scSTATseq method. UMAP clustering of the cells readily identified two prominent clusters of cells of similar size (Fig2A), and marker analysis demonstrated that cluster0 was composed of antigen-experienced effector cells positive for the effector molecules IFNG and GZMB, while cluster1 included naïve/memory cells that displayed high levels of CCR7 and S1PR1 (Fig2B). Pseudotime trajectory mapping based on the dispersed genes yielded a relatively simple arc, with the effector cells being assigned higher pseudotime values along this reference trajectory (Fig2C). We then generated iterated trajectory mappings using the curated hallmark signatures from three separate knowledgebases (Msigdb, KEGG, Reactome), and performed paired correlation analysis of the pseudotime values against the reference trajectory to identify pathways with close association and significant signal over noise based on gene set size (Fig2D). Consistent with our expectations, a relatively small portion of pathways showed significance, alleviating concerns about overfitting from our method (TableS1).

From direct inspection of the top pathways displaying significant association via TIPS analysis, we found a number of well-characterized processes known to influence CD8 behavior, such as chemokine signaling and IL12 family signaling (Fig2E). At the same time, we also observed significance in less appreciated processes such the Myd88-mediate TLR cascade and SLC-mediated transmembrane transport. Overall temporal alignment of these four pathways of interest based on the order of their switched-on genes demonstrated that each of these pathways had factors that changed across multiple points of the overall pseudotime trajectory, although most of the changes were centered at an intermediate timepoint marking a changeover from

memory to effector status (Fig2F). When we focused in on each pathway, we could observe that these changes included relatively critical constituents, such as the signaling kinase IRAK1 in the Myd88-mediated cascade. Many of these molecules have also previously been demonstrated to be of functional importance in the context of T cell immunity, such as the co-stimulatory molecule ICOS, the large neutral amino acid transporter SLC7A5, and the chemokine receptor CXCR1 [23-25]. We also recovered several interesting molecules not characterized in this context, such as the iron exporter ferroportin (SLC40A1) and zinc importer SLC39A2. Taken together, these results demonstrate that the TIPS workflow can successfully recapitulate existing knowledge of a biological context while also yielding novel candidates for further validation.

In order to put these pathway inferences relating to CD8+ T cells in context, we also further analyzed three additional scRNAseq datasets of CD8+ T cells generated using other library construction methods. From direct inspection, we noted that of the pathways of interest we described above, four were found to be conserved across at least 3 of the 4 datasets, with particularly strong conservation of the chemokine signaling pathway we highlighted (FigS1). This conservation could be found despite sharp differences between datasets in terms of information recovered. For instance, we could observe sharp differences in dropout rate and background noise levels between the scSTATseq and 10X libraries (FigS2). As such, we believe that the pathway inferences drawn through TIPS may be reproducible across multiple independent datasets.

Individual Gene Selection

In the results described above, we relied on picking genes with significant changes in switch-like expression as representative genes in a given pathway. However, it is well appreciated that not all genes may display this type of expression characteristic. As such, in order to develop a broader mechanism for identifying critical genes in a given pathway, we further explored using two other scoring approaches to assess gene significance. One approach is to perform a direct Pearson correlation between gene expression level for each cell with its assigned pseudotime, to capture genes with steady and monotonic expression changes. The other is to further iterate the DDRTree algorithm on a pathway-level, and calculate the impact removing a single given gene would have on the strength of the pseudotime correlation (DDRTree influence). When applied to the simulated dataset described above, we found that the correlation metric was highly associated with the switchde-based results, and did not help to discover more significantly associated genes (FigS3A). However, we found that the DDRTree influence metric recovered an independent pool of genes that did not follow switch-like behavior (FigS3C). These results were even more pronounced when applied to real data, as assessing DDRTree influence led to the identification of genes with complex expression dynamics (alternatively increasing then decreasing) (FigS4). Since these two metrics captured distinct pools of genes that are meaningful in different context, we elected to incorporate both of these methods for gene selection to help maximize the amount of information obtainable from TIPS and assist in downstream screening.

TIPS analysis of complex progression trajectories

While differentiation trajectories may sometimes involve a simple progression from one dominant state to another, real biological trajectories are oftentimes more complex, and involve multiple stable intermediate states. In order to understand if the TIPS workflow is sufficiently robust to handle these complex trajectories, we next applied it to analyze the differentiation trajectory of CD8+ tumor-infiltrating lymphocytes (TILs). TILs reside in a complex tumor-immune microenvironment, wherein different types of cellular and metabolic interactions may influence their behavior. CD8+ TILs in particular have been demonstrated to become functionally exhausted in many types of solid tumors, and prevention/reversal of exhaustion has been the focus of intensive research. To examine the processes underlying CD8+ TIL behavior, we applied the TIPS workflow to a dataset of CD8+ TILs derived from hepatocellular carcinoma (HCC) patients that was generated using the plate-based SMARTseq2 library construction.

From our initial dimension reduction via UMAP, we were able to observe a number of separate clusters that roughly corresponded to the published cellular annotations (Fig4A). These cell types progressed in our trajectory analysis in a somewhat irregular manner, with an undefined population of cells marking the pseudotime endpoint (Fig4B-C). A relatively small portion of curated pathways (51/1,114) were found to have significant association with this trajectory (TableS2), from which we could identify a few pathways that have been previously validated, such as receptor-tyrosine kinase (RTK) signaling and TLR cascade (Fig4D-E). From further exploration of the unannotated cluster, we found that the cluster was dominated by ribosomal signatures, explaining the inclusion of significant correlations with ribosome-related pathways in our inference (FigS5). More interestingly however, we also uncovered pathways that have been reported to influence CD8+ T cell behavior in other contexts, such as the ROBO receptors and ERBB2 signaling pathways [26-27]. These pathways largely underwent substantial changes in gene expression early on in the pseudotime trajectory, although a portion of the ROBO receptor pathway shifted later on (Fig4F). Manual inspection of the genes within these pathways demonstrated that while the expression of ROBO receptors themselves did not show strong changes with respect to pseudotime, we could observe increases in the chemokine receptor CXCR4 that has been shown to rely on ROBO cooperation (Fig4I). Similarly, while ERBB2 itself did not show significant changes in expression, we did note a decreased expression in its downstream signal mediator KRAS at the endstage of the pseudotime trajectory (Fig4J). Taken together, these results suggest that both of these pathways may also play significant roles in regulating CD8+ TIL behavior.

TIPS analysis of CD8+ TIL trajectory during checkpoint blockade

The recent development of immune checkpoint blockade (ICB) antibodies targeting PD-1/PD-L1 and CTLA-4 has opened a new avenue for cancer therapy. While these inhibitors are expected to have a significant impact on the behavior of TILs, the exact molecular mechanisms and processes that are altered as a result of their application are not yet fully understood. To

extend our analysis of TIL behavior in HCC from above, we next analyzed a droplet-based dataset of TILs taken from patients who had undergone direct surgical resection only, or otherwise received anti-PD-L1 and anti-CTLA4 or anti-PD-1 treatment prior to resection. After subsetting out the population of CD8+ T cells from the dataset, we observed from dimension reduction that there was substantial separation between cells taken from the patients who had received differential treatment. This separation was also clear in our trajectory construction, where cells derived from untreated patients marked the end stage, while those from patients treated with anti-PD-L1 and anti-CTLA4 marked the start point.

Application of TIPS using the Reactome and KEGG knowledgebase once again yielded a small pool of (52 out of 965) pathways with significant associations (TableS3). As a whole, these pathways were significantly different from those recovered from the previous analysis of HCC samples above. However, we were able to recover pathways such as cellular senescence and TCA cycle, which have been previously implicated to be altered as a result of ICB [28,29] (FigS6). At the same time, we also uncovered a number of pathways that have not characterized in this context, such as WNT signaling and estrogen-dependent gene expression. Whether these pathways and their downstream molecules may also be important contributors to ICB success remains an open question for future validation.

Discussion

While a large number of methods have been developed in recent years to help order cells along a single and/or multiple trajectories, obtaining information of biological significance of from such analysis has somewhat lagged behind [30]. In particular, although it has been demonstrated through a number of methods that trajectory analysis can recapitulate the known order of cellular maturation over the course of hematopoiesis, few studies have been able to discover novel transcription factors and/or biological processes that influence this process. In an attempt to redress this deficiency, we have presented the TIPS framework as described above to help uncover these molecular mechanisms. By relying on pseudotime trajectories as our point of comparison, we can maintain the single-cell nature of the data, and thereby identify pathways that change across multiple clusters. Furthermore, we can leverage existing tools for identifying gene changes with respect to pseudotime to give an overview of the temporal order in which pathways undergo significant changes. This latter form of temporal information is an additional vantage point that may of particular use in examining interdependent pathway relationships.

Although our current pseudotime workflow is built upon the DDRTree algorithm implemented in Monocle, we believe that this approach is not limited to this method for pseudotime assignment. Instead, the relative simplicity of our conceptual framework should allow it to be readily implemented using other algorithms, including those that enable simultaneous consideration of independent and/or circular trajectories. This flexibility thus allows for further optimization of pathway analysis methods for single cell data that have faster runtimes and potentially improved accuracy. We hope to be able to continually update our TIPS

server to incorporate these newer methods for pseudotime assignment. Similarly, we currently rely on the switchde concept of finding genes with single, abrupt changes in expression, to define the order at which a pathway may be activating. This approach may be particularly suitable for genes with pronounced burst [31]. However, not all genes will follow this pattern of expression; some may have substantially more gradual increases in response to stimuli as a result of a higher basal level of expression, while others may display more complex expression kinetics with multiple on/off switch points. Further development of gene kinetic modeling and regulatory inference algorithms may be able to identify ways to successfully capture the signal of these genes with respect to pseudotime and help refine our understanding of pathway kinetics [32].

In short, our conceptual approach is not limited by the type of single-cell library construction method used; we present worked examples of TIPS analysis as performed on three different datasets from independent sources and generated with different workflows. These datasets vary significantly in the numbers of cells sequenced, the numbers of genes detected per cell, and in their rate of technical dropout. This latter source of variation may have particularly significant ramifications on the accuracy of pseudotime alignment. A number of informatics tools have been designed to impute and correct for this variation [33]. However, as further advances in library construction lead to increasingly precise and accurate single-cell profiles, technical dropout may also be significantly ameliorated. Together with further refinement and expansion of knowledgebase data, we anticipate that the analytical framework we describe in this manuscript will only improve in accuracy and predictive power over time.

Key Points

- The TIPS framework can be used to infer which biological pathways are significantly associated with progression along a central pseudotime trajectory
- Additional contextual information on the relative order of pathway changes, and the specific genes driving such changes, can also be identified
- TIPS opens up new modes of information recoverable from trajectory analysis

Acknowledgements

The authors would like to thank the other members of lab for their constructive feedback during discussion and writing of this manuscript. In addition, the authors thank Prof. Haitao Li (Southwest University, Chongqing) for assistance in the production and purification of the Tn5 transposase used in library construction for scSTATseq.

Funding

This work was supported in part by National Key Project of China (2017YFA0700404 and 2016YFA0502201) to W.Y. and Natural Science Foundation of Shenzhen (JCYJ20190808150009605) to S.J.

Data Availability

All publicly available scRNAseq data analyzed in this study are available through GEO under the accessions GSE133535 (CD8+ T cell libraries constructed using other methods), GSE98683 (SMARTseq2 sequencing of CD8+ TILs from HCC patients), and GSE125449 (10X Genomics sequencing of CD8+ TILs from HCC patients after immune checkpoint blockade). scSTATseq sequenced libraries of CD8+ T cells will be made available through the Genome Sequence Archive (accession pending).

Figure 1—Overview of TIPS workflow

The TIPS workflow as presented here and as implemented in our GUI and shiny app requires the input of only a gene expression file and the selection of a reference database for consideration, with an optional option for helping visualize associated metadata. These data are then loaded to create a Seurat object. Three modes of dimension reduction are then run (PCA, tSNE, and UMAP) to generate 2-D visualizations of transcriptional similarity between cells using HVGs. A trajectory is constructed using DDRTree in monocle (run in successive order in our app). Users may then select parameters regarding gene size and expression to filter for pathways of interest, and additional trajectories are then constructed based on individual pathway gene sets. The statistical significance of each pathway is computed based on signal relative to background noise from 1,000 randomly selected gene lists of the same size. Users may then further select specific pathways of interest for further analysis. These analyses include temporal ordering of different pathways, as well as selection of the critical genes from each pathway for downstream validation. All visualizations can be exported as publication-ready PDFs or tiffs with selectable scaling. The Seurat and monocle objects are stored in a directory to allow for further manipulation by the user if necessary. Full tables of pathways and genes within displaying significant association are also provided as text files.

Figure 2—Parameter Testing using Simulated Data

For parameter testing, we used a simulated dataset of 500 cells and 5,000 genes per cell, comparable in information amount to most real single-cell datasets. We then generated 1,000 lists of 100 genes each for background measurement, and 100 lists of 100 genes each from the subset of HVGs (527 total) as our signal of interest. A) Average gene expression is commonly used as a metric for identifying significantly associated pathways in bulk analyses. However, no differences in correlation distribution could be found when HVG lists and random lists were compared using averaged expression to pseudotime correlation. B) When the lists were instead run through DDRTree to generate individual pseudotime vectors, pseudotime vectors derived from HVG lists showed very high levels of correlation, while few random lists showed significance. P values shown in A and B are for the Pearson correlation statistic. C) Dotplot of pseudotime correlation vs expression correlation demonstrates that the majority of HVG lists that showed high levels of pseudotime correlation had very little correlation in terms of expression (R <0.2). D) Dotplot of the expression profiles of all HVGs of the simulated dataset derived from switchde. *mu0* indicates the half-peak expression of a gene prior to the switch event, while *k* indicates the magnitude of the switch event, and *t0* the timepoint along the trajectory at which the switch event takes place. We can observe that most of the genes displaying noticeable switch behavior had low average expression, but roughly equal numbers of genes had increasing or decreasing expression. E) Taking one significantly associated HVG list as an example, we can observe that a given pathway may also include individual genes with increasing and decreasing

expression. F) By increasing or decreasing the size of the gene list considered, we can observe that the magnitude of the pseudotime correlation is highly sensitive to the size and amount of information considered. When the top50 genes with increasing expression by switchde are considered, the resulting correlation is higher than if the next 51 (top51-101) are considered. However, the full list of top100 genes has a higher correlation still. This effect can also be seen in the genes with decreasing expression (bot1-100). Furthermore, a fuller list of 200 genes (union of the top100 increasing and bottom100 decreasing) has a higher correlation than either list alone. These results confirm that the method is sufficiently sensitive. G) Real scRNAseq datasets can vary greatly in the numbers of cells sequenced. By subsetting the simulated set, we sought to measure the influence of changes in dataset size. Interestingly, while the smaller sets did display reduced correlation between the new pseudotime assignments for the cells subsetted and their original pseudotime values, most subsets retained a representative capability with $R > 0.9$ at 50 cells. H) Real scRNAseq may also display zero-inflation as a result of technical dropout or transcriptional burst. By artificially adding in zero-inflation to splatter, we observed that an increase in dropout could drive a sharp decrease in pseudotime correlation. Indeed, past a certain threshold, trajectory analysis would be essentially meaningless. I) Real scRNAseq datasets may also measure and consider gene sets of different sizes. By changing the size of a randomly selected gene set, we also observed significant changes in the distribution of pseudotime correlation values; larger datasets naturally tended to have higher noise.

Figure 3—TIPS workflow applied to CD8+ T cells

A) UMAP reduction and clustering of the sorted CD8+ T cells identifies two prominent clusters reflective of effector and naïve/memory like populations. B) Violin plot of four prominent markers of T cell state demonstrate that the effector cluster features high expression of the functional molecules *GZMB* and *IFNG*, while the memory cluster shows elevated expression of *CCR7* and *S1PR1*. C) Trajectory mapping of these cells reveals a simple arcing path with ordered progression from memory to effector cells. D) Volcano plot of the distribution of pseudotime correlation values and false discovery rates (FDR) for all pathways derived from three databases considered. Notably, a number of larger pathways do display high levels of pseudotime correlation, but at a level functionally indistinguishable from randomly selected gene sets of matching size. E) Dotplot visualization of ten pathways of interest that had significant correlation. While TIPS includes a default option for picking the top10 pathways, users may also wish to highlight specific pathways of interest. F) Temporal ordering of four pathways of interest using the switch points of significant genes along the trajectory. While the majority of the switch events occur at the point of change between memory and effector populations, a significant portion also occur at earlier and later points, indicating that the changes do not simply describe DEGs between the two clusters. G-J) Plots of the scaled expression of specific genes of interest from each pathway visualized over the course of pseudotime progression. These include genes that changed late in the trajectory, such as *CXCR1* from the chemokine signaling pathway, as well as genes that change earlier on, such as *IL12A* from the IL-12 family signaling pathway.

Figure 4– Application of TIPS to identify pathways associated with CD8 TIL function

A) UMAP reduction of the subset of CD8+ TILs taken from tumor regions (annotated as TTC in original data) shows relatively clean separation between the 5 types of annotated cell populations described in the original analysis, with some overlap caused by differences in dimension reduction method and HVG selection. B-C) Trajectory mapping of these cells shows some stratification between cell states along the pseudotime trajectory, with a relatively prominent placement of unannotated cells at the end point of the trajectory. D) Distribution of pathways according to pseudotime correlation and FDR shows relatively few significant pathways. E) Dotplot visualization of several significant pathways. F) Temporal ordering of selected pathways shows that most changes occur early on along the trajectory, although the ROBO receptors pathway includes a secondary peak of changes at the middle of the trajectory. G-J) Plots of the scaled expression of specific genes of interest from each pathway visualized over the course of pseudotime progression.

FigS1—Conservation of TIPS results in other CD8+ T scRNAseq datasets

A) Dotplot of the pseudotime correlations found in each independent dataset for ten pathways of interest inferred to be significantly associated in the scSTATseq dataset. SMARTseq3, scSTATseq, and Quartzseq2 are all plate-based methods for library construction, while the 10X chromium technique is the currently most common droplet-based method. B) The relative proportion of the genes in each pathway found to be measured in each dataset. Notably, while SMARTseq3 and scSTATseq generally detect expression of large portions of these genes, the Chromium and Quartzeq2 data show lower detection rates, likely explaining the sharp differences in correlation.

FigS2—In-depth comparison of plate and droplet-based sequencing quality

A) Overall dropout rate was much higher in the droplet-based library, as fewer than 2,000 genes were found in more than 50% of the cells, while over 10,000 genes were found at over 50% detection in the plate-based library. B) Because of this zero-inflation dropout, the droplet-based library has very high coefficient of variation (CV) for genes with low levels of average expression. C) Further inspection showed that the droplet based library has a tendency of aligning pseudotime trajectory in an order from cells with fewer genes to cells with more genes. This intrinsic effect has significant consequences on the level of background noise. D-E) While background noise in both droplet-based and plate-based data increase based on the numbers of genes considered (1,000 randomly selected lists for each size), the rate of increase was substantially more dramatic in the droplet-based data. F-G) This effect also caused the droplet-based data to have high correlation between expression level and pseudotime correlation, a phenomenon not seen in the plate-based data.

FigS3—Gene selection in simulated data

Single gene correlation with the overall pseudotime trajectory, the intensity of single gene switching, and the influence of a single gene on DDRTree correlation were computed for a pool of 100 HVGs. A-C) Intensity of switch events and expression correlation showed significant correlation. However, DDRTree influence was significantly independent from these two metrics. D-E) Top5 genes selected based on their magnitude of DDRTree influence or switch intensity shows no pronounced differences.

FigS4—Gene selection in real data

Single gene correlation with the overall pseudotime trajectory, the intensity of single gene switching, and the influence of a single gene on DDRTree correlation were computed for a pool of genes in the chemokine signaling pathway. A-C) Intensity of switch events and expression correlation showed significant correlation as in the simulated set. However, DDRTree influence was significantly independent from these two metrics. D-E) Top5 genes selected based on their magnitude of DDRTree influence or switch intensity. Whereas the genes selected based on switch-like behavior tend to display a singular change in expression, genes selected based on DDRTree influence feature multiple peaks indicative of more complex expression dynamics.

FigS5—Annotation of an originally unannotated cluster of cells

A) From our trajectory analysis, we also observed a number of pathways representing ribosomal activity and basic transcription/translation to be significantly associated with the overall trajectory. B) Heatmap of the top cluster-unique genes in the unknown cluster demonstrates that the cluster is dominated by a ribosomal signature.

FigS6-- Application of TIPS to identify pathways responsive to checkpoint blockade

A) UMAP reduction of the subset of CD8+ TILs taken from tumor regions shows clean separation between cell signatures as a result of ICB blockade treatment. B-C) Trajectory mapping of these cells shows some stratification between cell states along the pseudotime trajectory, with cells from untreated patients reaching the end of the trajectory. D) Distribution of pathways according to pseudotime correlation and FDR shows relatively few significant pathways. E) Dotplot visualization of several significant pathways. F) Temporal ordering of selected pathways shows that most changes occur throughout the trajectory, with the estrogen-dependent expression pathway more prominently featured at the end of the trajectory. Notably, we could also observe early changes in genes associated with cellular senescence.

References

[1] Aibar S, González-Blas CB, Moerman T, et al. SCENIC: single-cell regulatory network inference and clustering. Nat Methods. 2017 Nov;14(11):1083-1086. doi: 10.1038/nmeth.4463.

[2] La Manno G, Soldatov R, Zeisel A, et al. RNA velocity of single cells. Nature. 2018 Aug;560(7719):494-498. doi: 10.1038/s41586-018-0414-6.

[3] Efremova M, Vento-Tormo M, Teichmann SA, et al. CellPhoneDB: inferring cell-cell communication from combined expression of multi-subunit ligand-receptor complexes. Nat Protoc. 2020 Apr;15(4):1484-1506. doi: 10.1038/s41596-020-0292-x.

[4] Lähnemann D, Köster J, Szczurek E, et al. Eleven grand challenges in single-cell data science. Genome Biol. 2020 Feb 7;21(1):31. doi: 10.1186/s13059-020-1926-6.

[5] Andrews TS, Hemberg M. False signals induced by single-cell imputation. Version 2. F1000Res. 2018 Nov 2 [revised 2019 Mar 5];7:1740. doi: 10.12688/f1000research.16613.2.

[6] Baran Y, Bercovich A, Sebe-Pedros A, et al. MetaCell: analysis of single-cell RNA-seq data using K-nn graph partitions. Genome Biol. 2019 Oct 11;20(1):206. doi: 10.1186/s13059-019-1812-2.

[7] Aibar. et al. (2016) AUCell: Analysis of 'gene set' activity in single-cell RNA-seq data. R/Bioconductor package.

[8] Hänzelmann S, Castelo R, Guinney J. GSVA: gene set variation analysis for microarray and RNA-seq data. BMC Bioinformatics. 2013 Jan 16;14:7. doi: 10.1186/1471-2105-14-7.

[9] Kanehisa M, Sato Y. KEGG Mapper for inferring cellular functions from protein sequences. Protein Science. doi: 10.1002/pro.3711

[10] Jassal B, Matthews L, Viteri G., et al. The reactome pathway knowledgebase. Nucleic Acids Res. 2020 Jan 8;48(D1):D498-D503. doi: 10.1093/nar/gkz1031.

[11] Subramanian A, Tamayo P, Mootha VK, et al. Gene set enrichment analysis: a knowledge-based approach for interpreting genome-wide expression profiles. Proc Natl Acad Sci USA 2005 Oct 25;102(43):15545-50. doi: 10.1073/pnas.0506580102.

[12] Butler A, Hoffman P, Smibert P, et al. Integrating single-cell transcriptomic data across different conditions, technologies, and species. Nat Biotechnol. 2018 Jun;36(5):411-420. doi: 10.1038/nbt.4096.

[13] Becht E, McInnes L, Healy J, et al. Dimensionality reduction for visualizing single-cell data using UMAP. Nat Biotechnol. 2018 Dec 3. doi: 10.1038/nbt.4314.

[14] Trapnell C, Cacchiarelli D, Grimsby J, et al. The dynamics and regulators of cell fate decisions are revealed by pseudotemporal ordering of single cells. Nat Biotechnol. 2014 Apr;32(4):381-386. doi: 10.1038/nbt.2859.

[15] Campbell KR, Yau C. switchde: inference of switch-like differential expression along single-cell trajectories. Bioinformatics. 2017 Apr 15;33(8):1241-1242. doi: 10.1093/bioinformatics/btw798.

[16] Wehrens R and Kruisselbrink J. Flexible Self-Organizing Maps in kohonen 3.0. Journal of Statistical Software, 2018 *87*(7), pp. 1-18. doi: 10.18637/jss.v087.i07

[17] Zappia L, Phipson B, Oshlack A. Splatter: simulation of single-cell RNA sequencing data. Genome Biol. 2017 Sep 12;18(1):174. doi: 10.1186/s13059-017-1305-0.

[18] Zheng Z, Tang X, Qiu X, et al. scSTATseq: Diminishing Technical Dropout Enables Core Transcriptome Recovery and Comprehensive Single-cell Trajectory Mapping. Preprint: Biorxiv. doi: 10.1101/2020.04.15.042408

[19] Patro R, Duggal G, Love MI, et al. Salmon provides fast and bias-aware quantification of transcript expression. Nat Methods. 2017 Apr;14(4):417-419. doi: 10.1038/nmeth.4197.

[20] Mereu E, Lafzi A, Moutinho C, et al. Benchmarking single-cell RNA-sequencing protocols for cell atlas projects. Nat Biotechnol. 2020 Jun;38(6):747-755. doi: 10.1038/s41587-020-0469-4.

[21] Zhang Q, He Y, Luo N, et al. Landscape and Dynamics of Single Immune Cells in Hepatocellular Carcinoma. Cell. 2019 Oct 31;179(4):829-845.e20.doi: 10.1016/j.cell.2019.10.003.

[22] Ma L, Hernandez MO, Zhao Y, et al. Tumor Cell Biodiversity Drives Microenvironmental Reprogramming in Liver Cancer. Cancer Cell. 2019 Oct 14;36(4):418-430.e6. doi: 10.1016/j.ccell.2019.08.007.

[23] Wallin JJ, Liang L, Bakardjiev A, et al. Enhancement of CD8+ T cell responses by ICOS/B7h costimulation. J Immunol. 2001 Jul 1;167(1):132-9. doi: 10.4049/jimmunol.167.1.132.

[24] Hess C, Means TK, Autissier P, et al. IL-8 responsiveness defines a subset of CD8 T cells poised to kill. Blood. 2004 Dec 1;104(12):3463-71. doi: 10.1182/blood-2004-03-1067.

[25] Sinclair LV, Howden AJ, Brenes A, et al. Antigen receptor control of methionine metabolism in T cells. Elife. 2019 Mar 27;8:e44210. doi: 10.7554/eLife.44210.

[26] Prasad A, Qamri Z, Wu J, et al. Slit-2/Robo-1 modulates the CXCL12/CXCR4-induced chemotaxis of T cells. J Leukoc Biol. 2007 Sep;82(3):465-76. doi: 10.1189/jlb.1106678.

[27] Lozano T, Chocarro S, Martin C, et al. Genetic Modification of CD8(+) T Cells to Express EGFR: Potential Application for Adoptive T Cell Therapies. Front Immunol. 2019 Dec 20;10:2990. doi: 10.3389/fimmu.2019.02990.

[28] Im SJ, Hashimoto M, Gerner MY, et al. Defining CD8+ T cells that provide the proliferative burst after PD-1 therapy. Nature. 2016 Sep 15;537(7620):417-421. doi: 10.1038/nature19330.

[29] LaFleur MW, Nguyen TH, Coxe MA, et al. PTPN2 regulates the generation of exhausted CD8(+) T cell subpopulations and restrains tumor immunity. Nat Immunol. 2019 Oct;20(10):1335-1347. doi: 10.1038/s41590-019-0480-4.

[30] Saelens W, Cannoodt R, Todorov H, et al. A comparison of single-cell trajectory inference methods. Nat Biotechnol. 2019 May;37(5):547-554. doi: 10.1038/s41587-019-0071-9.

[31] Larsson AJM, Johnsson P, Hagemann-Jensen M, et al. Genomic encoding of transcriptional burst kinetics. Nature. 2019 Jan;565(7738):251-254. doi: 10.1038/s41586-018-0836-1.

[32] Pratapa A, Jalihal AP, Law JN, et al. Benchmarking algorithms for gene regulatory network inference from single-cell transcriptomic data. Nat Methods. 2020 Feb;17(2):147-154. doi: 10.1038/s41592-019-0690-6.

[33] Lan T, Hutvagner G, Lan Q. Sequencing dropout-and-batch effect normalization for single-cell mRNA profiles: a survey and comparative analysis. Brief Bioinform. 2020 Oct 19:bbaa248. doi: 10.1093/bib/bbaa248.

Gene Expression Matrix (.csv)

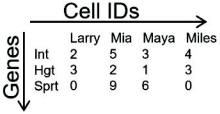

UMAP Clustering

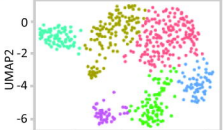

Pseudotime Correlation

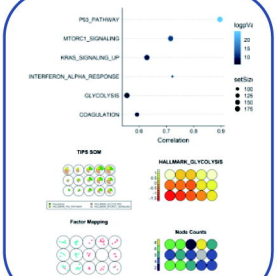

Temporal Ordering

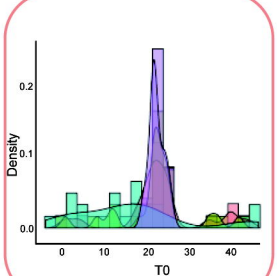

Sample Metadata (.csv)

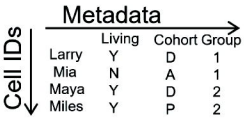

Trajectory Mapping

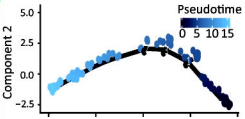

Background Control

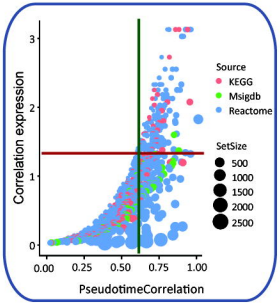

Gene-Pseudotime Alignment

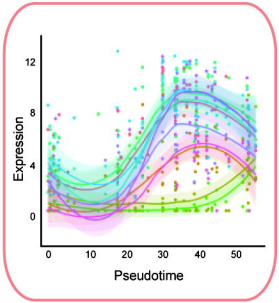

Reference Gene Sets (.gmt)

Pathway Iteration

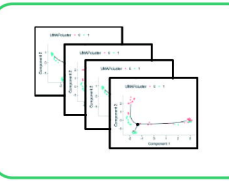

Data Input → **Initial Mapping** → **Pathway Identification** → **Detailed Selection**

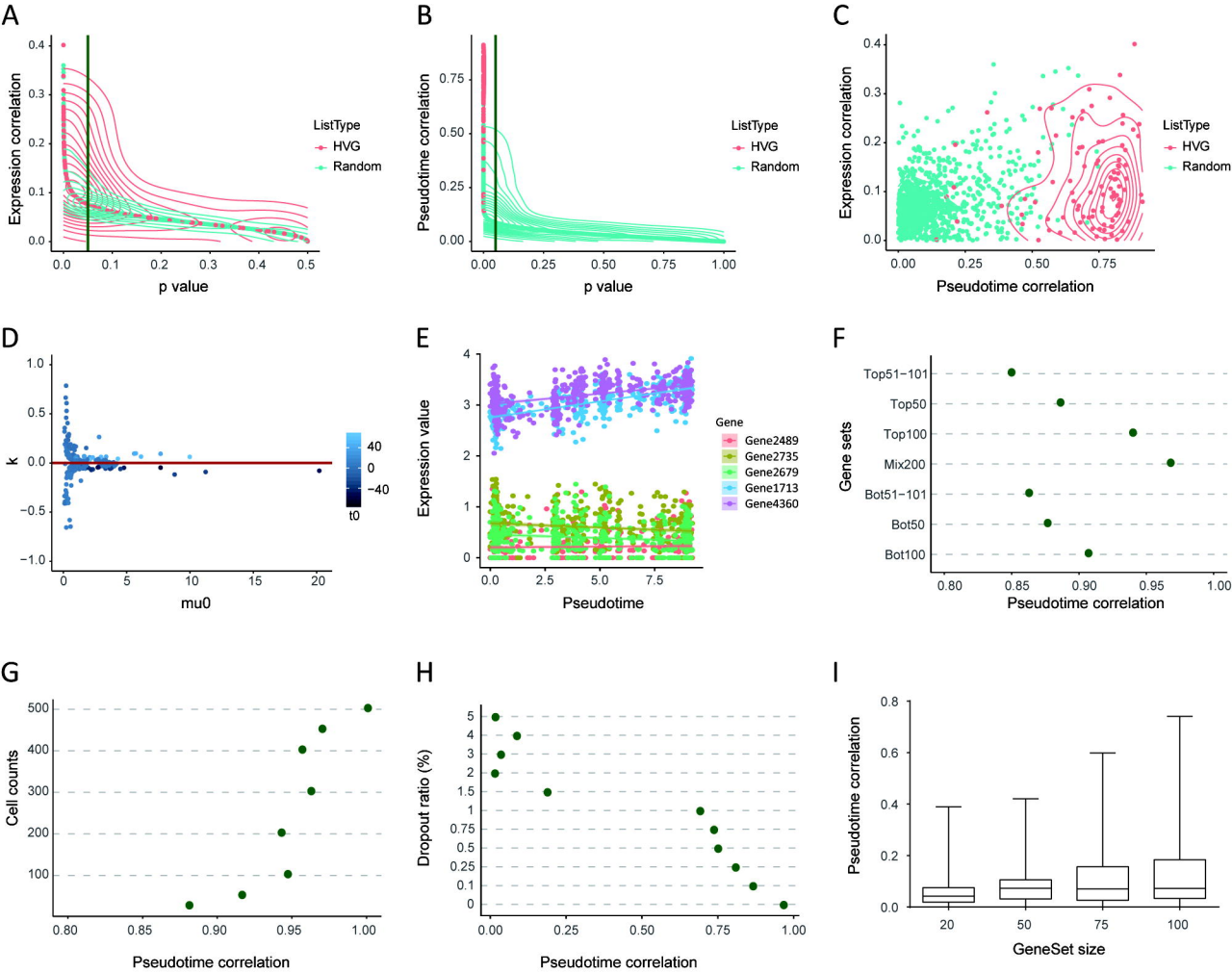
A
Expression correlation
p value
ListType
HVG
Random
B
Pseudotime correlation
p value
ListType
HVG
Random
C
Expression correlation
Pseudotime correlation
ListType
HVG
Random
D
k
mu0
t0
E
Expression value
Pseudotime
Gene
Gene2489
Gene2735
Gene2679
Gene1713
Gene4360
F
Gene sets
Top51−101
Top50
Top100
Mix200
Bot51−101
Bot50
Bot100
Pseudotime correlation
G
Cell counts
Pseudotime correlation
H
Dropout ratio (%)
Pseudotime correlation
I
Pseudotime correlation
GeneSet size

A

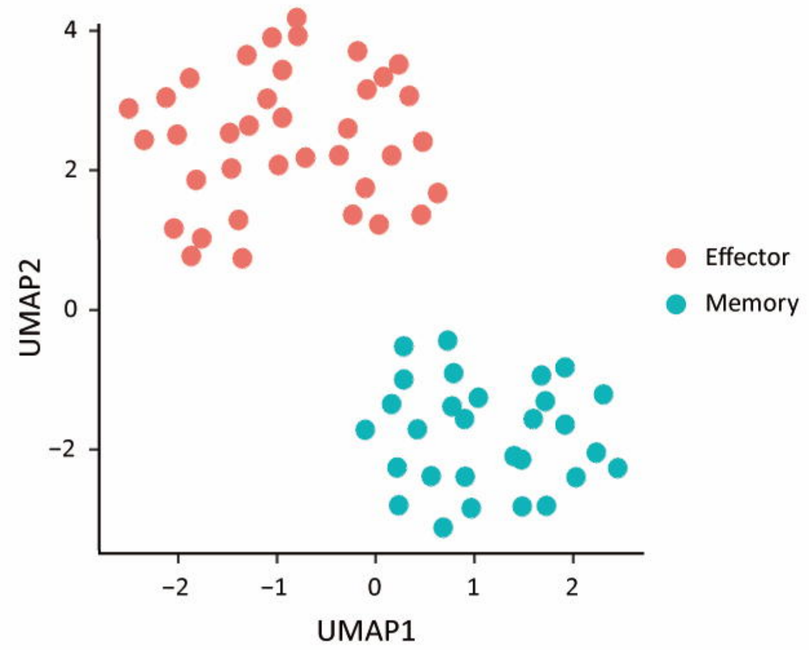

B

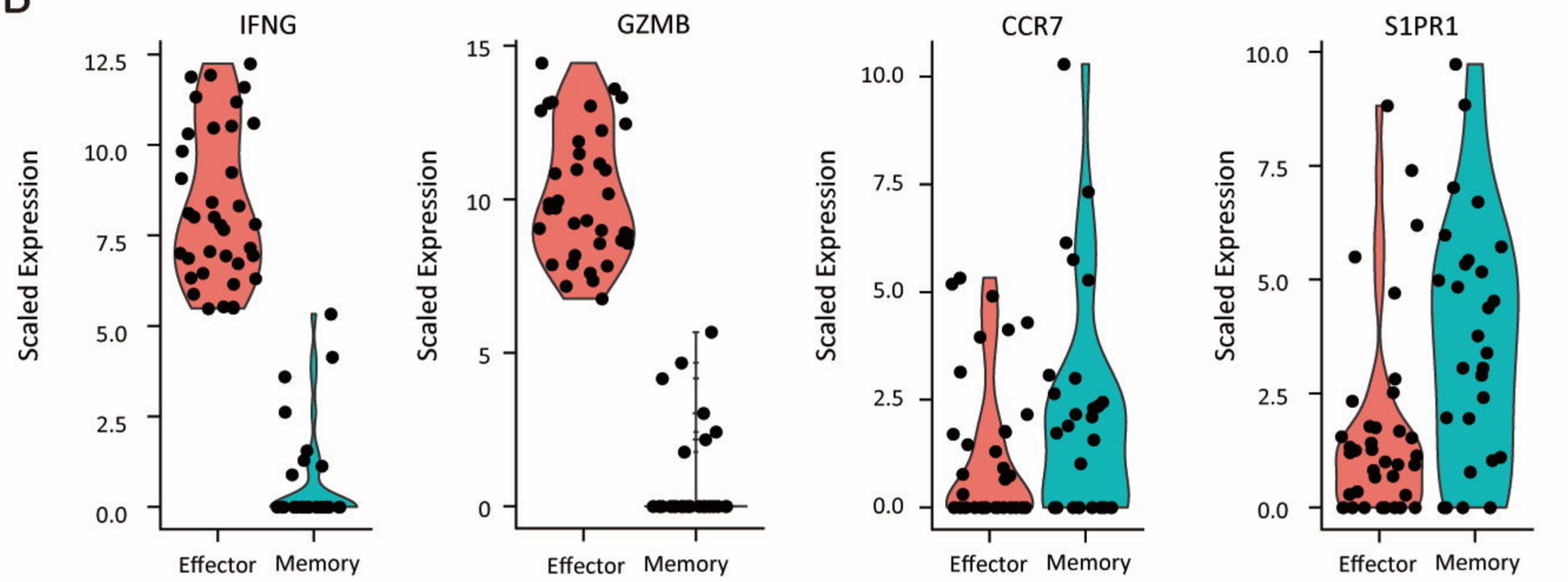

C

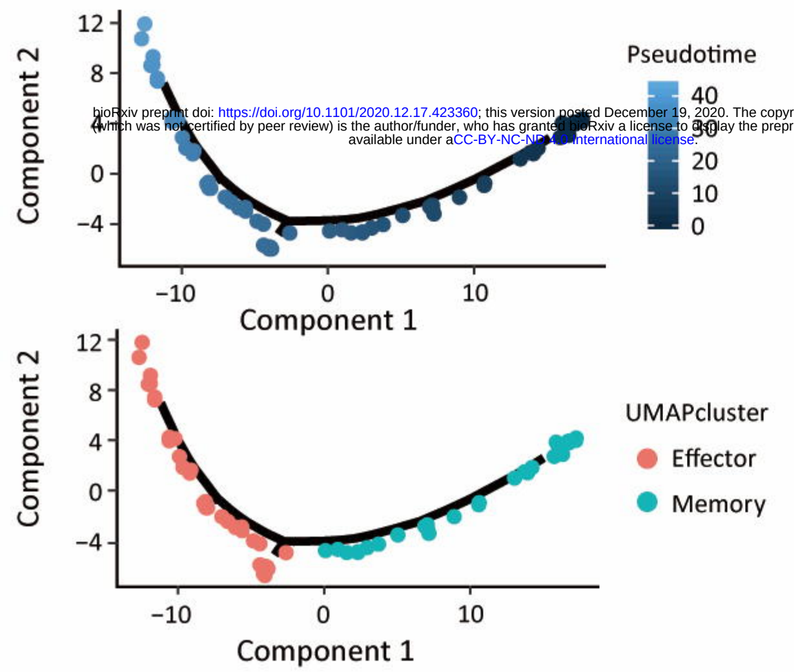

D

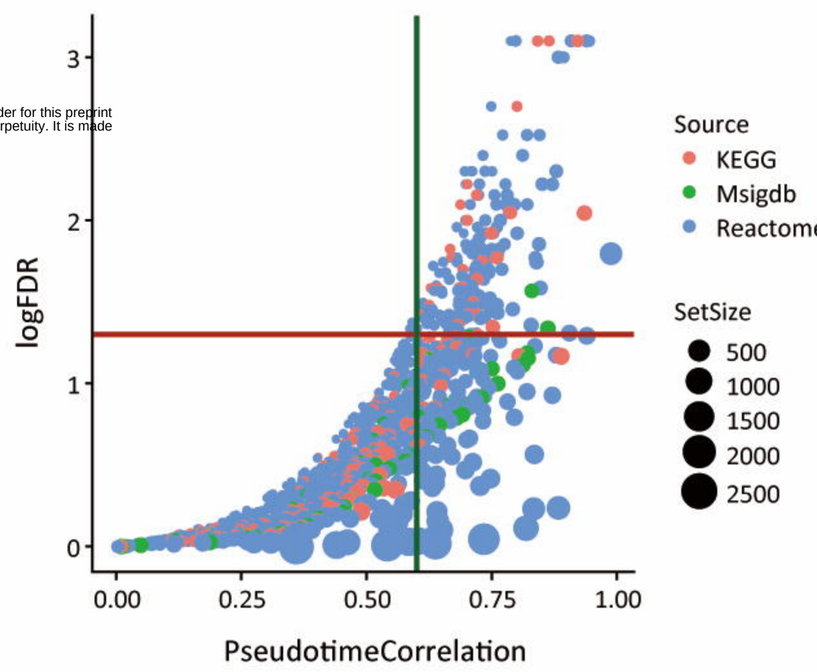

E

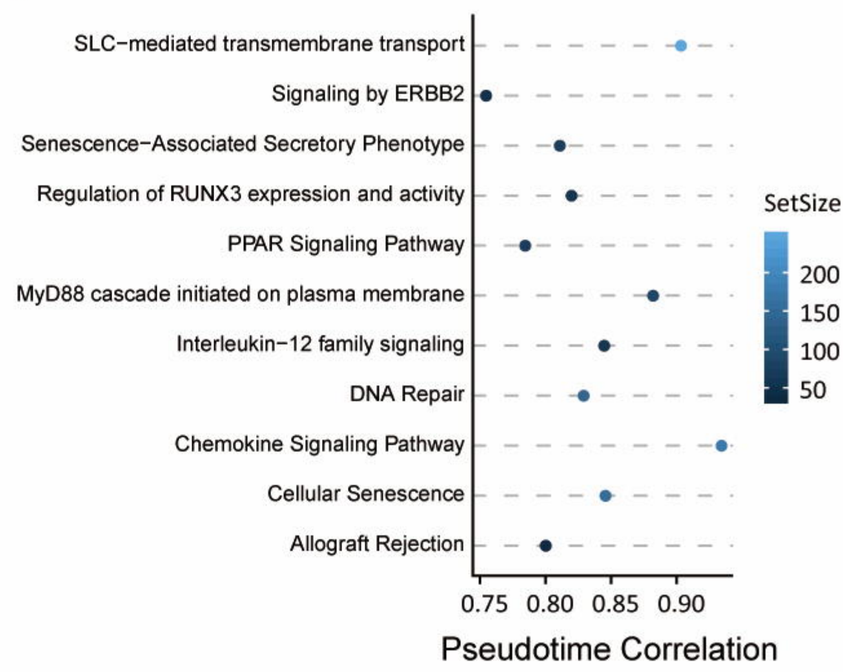

F

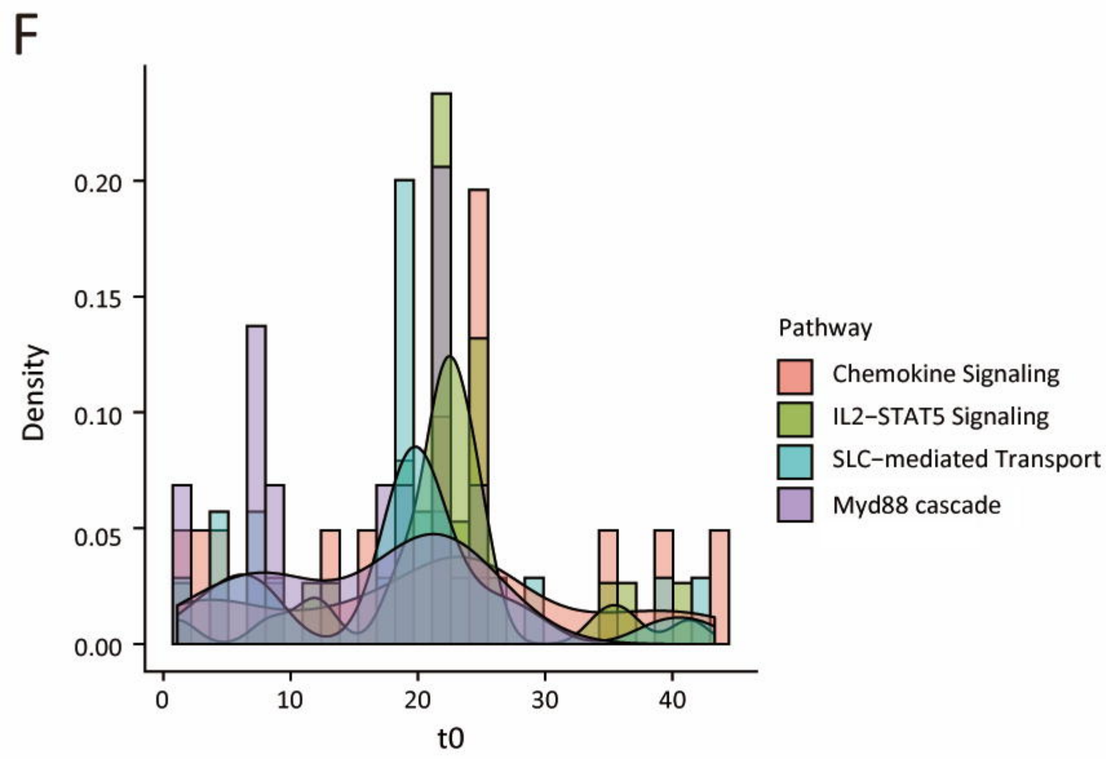

G

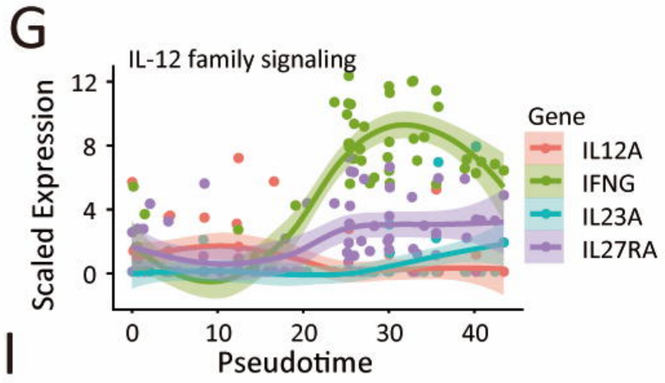

H

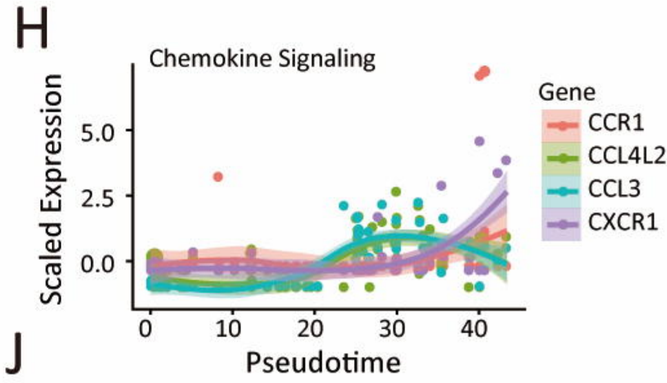

I

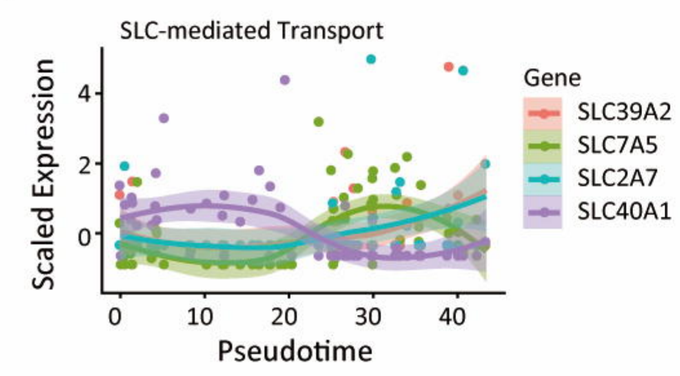

J

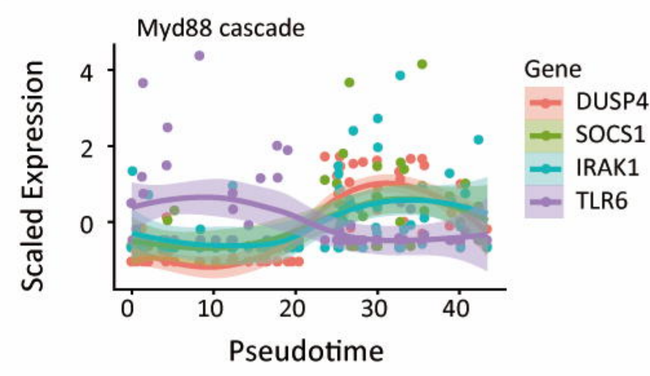

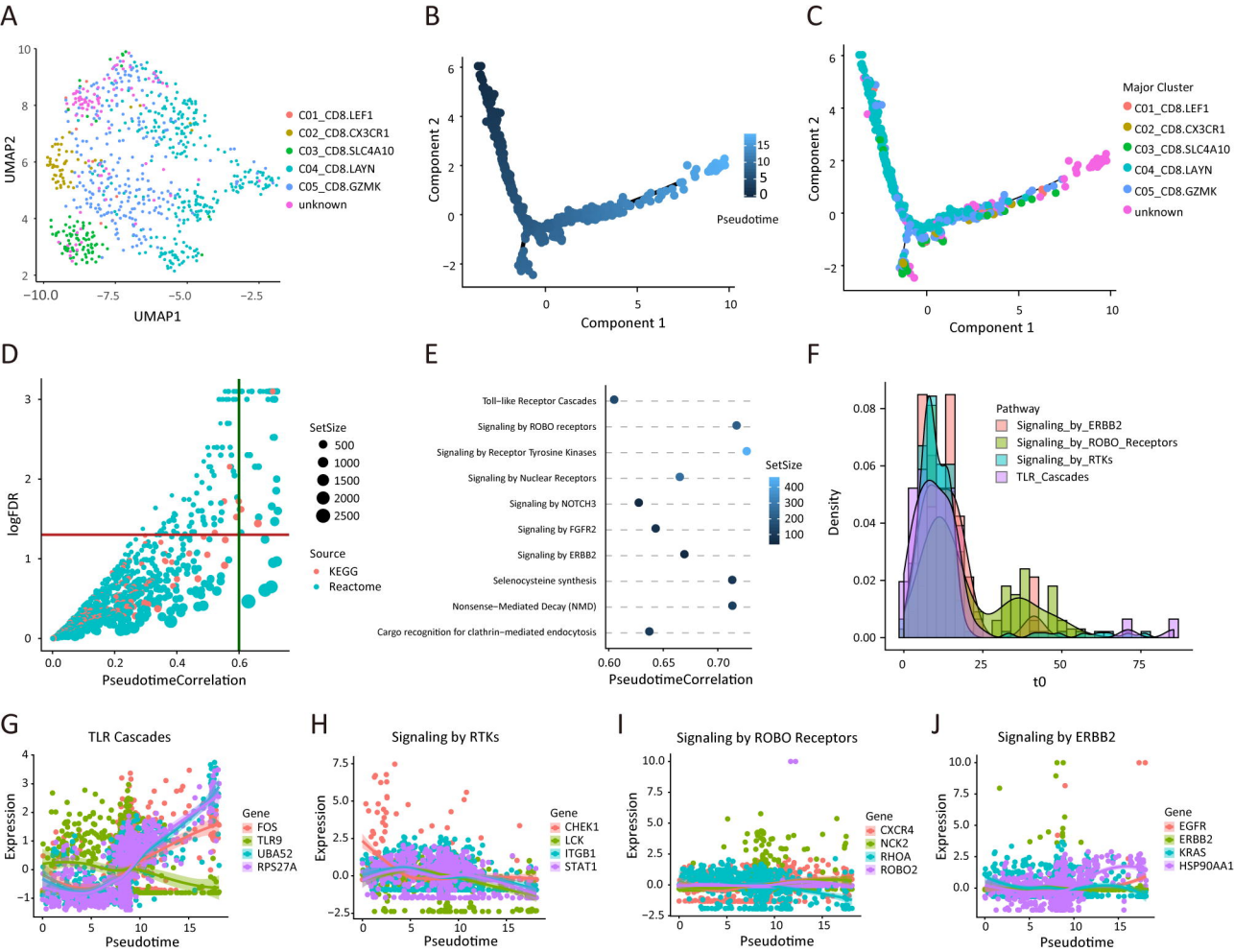
A
UMAP2
UMAP1
C01_CD8.LEF1
C02_CD8.CX3CR1
C03_CD8.SLC4A10
C04_CD8.LAYN
C05_CD8.GZMK
unknown
B
Component 2
Component 1
Pseudotime
C
Major Cluster
C01_CD8.LEF1
C02_CD8.CX3CR1
C03_CD8.SLC4A10
C04_CD8.LAYN
C05_CD8.GZMK
unknown
D
logFDR
PseudotimeCorrelation
SetSize
Source
KEGG
Reactome
E
Toll-like Receptor Cascades
Signaling by ROBO receptors
Signaling by Receptor Tyrosine Kinases
Signaling by Nuclear Receptors
Signaling by NOTCH3
Signaling by FGFR2
Signaling by ERBB2
Selenocysteine synthesis
Nonsense-Mediated Decay (NMD)
Cargo recognition for clathrin-mediated endocytosis
PseudotimeCorrelation
SetSize
F
Pathway
Signaling_by_ERBB2
Signaling_by_ROBO_Receptors
Signaling_by_RTKs
TLR_Cascades
Density
t0
G
TLR Cascades
Expression
Pseudotime
Gene
FOS
TLR9
UBA52
RPS27A
H
Signaling by RTKs
Expression
Pseudotime
Gene
CHEK1
LCK
ITGB1
STAT1
I
Signaling by ROBO Receptors
Expression
Pseudotime
Gene
CXCR4
NCK2
RHOA
ROBO2
J
Signaling by ERBB2
Expression
Pseudotime
Gene
EGFR
ERBB2
KRAS
HSP90AA1